

Short range ferromagnetism and spin glass state in $Y_{0.7}Ca_{0.3}MnO_3$

R. Mathieu and P. Nordblad

Department of Materials Science, Uppsala University, Box 534, SE -751 21 Uppsala, Sweden

D. N. H. Nam* and N. X. Phuc

Institute of Materials Science, NCST, Nghiado - Caugiay - Hanoi, Vietnam

N. V. Khiem

Department of Science and Technology, Hongduc University, Thanhhoa, Vietnam

(October 29, 2018)

Abstract

Dynamic magnetic properties of $Y_{0.7}Ca_{0.3}MnO_3$ are reported. The system appears to attain local ferromagnetic order at $T_{\text{SRF}} \approx 70$ K. Below this temperature the low field magnetization becomes history dependent, i.e. the zero field cooled (ZFC) and field cooled (FC) magnetization deviate from each other and closely logarithmic relaxation appears at our experimental time scales ($0.3\text{-}10^4$ sec). The zero field cooled magnetization has a maximum at $T_f \approx 30$ K, whereas the field cooled magnetization continues to increase, although less sharply, also below this temperature. Surprisingly, the dynamics of the system shows non-equilibrium spin glass (SG) features not only below the maximum in the ZFC magnetization, but also in the temperature region between this maximum and T_{SRF} . The aging and temperature cycling experiments show only quantitative differences in the dynamic behavior above and below the maximum in the ZFC-magnetization; similarly, memory effects are observed in both temperature regions. We attribute the high temperature behavior to the existence of clusters of short range ferromagnetic order below T_{SRF} ; the configuration evolves into a conventional spin glass state at temperatures below T_f .

*and Department of Materials Science, Uppsala University, Box 534, SE - 751 21 Uppsala, Sweden

I. INTRODUCTION

Magnetic frustration resulting from the competing coexistence of ferromagnetic double-exchange (DE) and antiferromagnetic superexchange interaction, is present in colossal magneto-resistance (CMR) materials. Recently, frustration related effects have been observed in the CMR ferromagnet $\text{Nd}_{0.7}\text{Sr}_{0.3}\text{MnO}_3$ ¹; also, a reentrant spin-glass (RSG) phase has been evidenced in $\text{La}_{0.96-x}\text{Nd}_x\text{K}_{0.04}\text{MnO}_3$ ² using relaxation measurements. In a recent paper³, SG-like behavior has been advocated in $\text{Y}_{0.7}\text{Ca}_{0.3}\text{MnO}_3$ from a cusp at $T \approx 30$ K in the $M_{\text{ZFC}}(T)$ curve and a corresponding frequency dependence in the ac susceptibility. In the present work, we have performed low-field magnetic relaxation and associated temperature cycling measurements at temperatures above and below the $M_{\text{ZFC}}(T)$ maximum. The relaxation of the low-frequency ac susceptibility is also studied to investigate memory effects in the two temperature regions. Below T_f the system exhibits features of a true SG state. However, long-time relaxation and aging effects are still found at higher temperatures, well above T_f . Additional magnetic hysteresis measurements reveal ferromagnetic short-range correlations below T_{SRF} , suggesting the existence of clusters of ferromagnetic order. Memory effects are observed in both regions.

II. SAMPLE AND EXPERIMENTS

The $\text{Y}_{0.7}\text{Ca}_{0.3}\text{MnO}_3$ (YCMO) compound was prepared by standard solid state reaction. After sintering at 1300° C, the mixture was annealed in oxygen at 1000, 800, and 600° C for several days at each temperature. The final product was characterized by x-ray diffraction technique showing a single phase of orthorhombic structure. The XRD measurements were performed at room temperature using a Siemens D5000 diffractometer with CuK_α radiation ($\lambda=1.5406$ Å) and a scanning step of 0.02°. The sample was first mixed with high-purity Si powder for standard angular calibration. As seen in the diffractogram presented in Fig. 1, which includes the Si peaks, the YCMO reflections can be indexed according to an orthorhombic structure. The obtained lattice parameters are $a=5.528$ Å, $b=7.441$ Å, and $c=5.293$ Å, in agreement with earlier results³. No secondary phases or impurities were detected.

The temperature dependence of the zero-field-cooled (ZFC), field-cooled (FC) and thermo-remanent (TRM) magnetization, as well as the relaxation of ZFC magnetization $m(t)$ and temperature cycling measurements⁴ were made in a non-commercial low field SQUID system⁵; the background field of which is less than 1 mOe. In the relaxation experiments, the sample was rapidly cooled in zero field from a reference temperature of 80 K to a measuring temperature T_m and kept there a wait time t_w . After the wait time, a small probing field H was applied and $m(t)$ was recorded as a function of the time elapsed after the field application. In the temperature cycling measurements, just after the wait time and immediately prior to the application of the probing field, the sample was additionally subjected to a temperature cycle ΔT of duration t_{w2} . Using the same SQUID system, low-frequency ac susceptibility experiments were used to investigate memory phenomena.

Additional “high field” measurements were performed in a commercial Quantum Design MPMS5 SQUID magnetometer (Curie Weiss behavior and Arrot plots) and a Lakeshore 7225 susceptometer (ac susceptibility in large superimposed dc-fields).

III. RESULTS AND DISCUSSION

A. Dc measurements

Figure 2 presents the $M_{\text{ZFC}}(T)/H$, $M_{\text{FC}}(T)/H$, and $M_{\text{TRM}}(T)/H$ curves measured at an applied field of 0.1 Oe. $M_{\text{ZFC}}(T)$ exhibits a maximum at $T_f \approx 30$ K in agreement with a previously reported result³. The inset shows the ZFC and FC curves for 0.1 and 0.5 Oe; a substantial suppression of $M_{\text{FC}}(T)/H$ is seen, whereas $M_{\text{ZFC}}(T)/H$ is virtually unaffected by the increased field strength. As demonstrated in Fig. 3(a), a Curie-Weiss behavior is observed at temperatures above $T_{\text{SRF}} \approx 70$ K. M_{TRM} appears nonzero below T_{SRF} and both $M_{\text{ZFC}}(T)$ and $M_{\text{FC}}(T)$ deviate from Curie-Weiss behavior suggesting an establishment of ferromagnetic correlations related to the double-exchange mechanism. However, our $M(H)$ measurements in applied fields up to 3 T and the corresponding Arrot plots (Fig. 3(b)) show no indication of spontaneous magnetization. These results imply that the ferromagnetism appearing below T_{SRF} is of short-range order, i.e. clusters of short-range FM correlations develop below T_{SRF} . Similar magnetic properties have previously been reported for $(\text{Tb}_{1/3}\text{La}_{2/3})\text{Ca}_{1/3}\text{MnO}_3$ wherein short-range ferromagnetic correlations above T_f were evidenced from magnetic and small-angle neutron scattering measurements⁶.

It is observed in our $m(t)$ measurements that $\text{Y}_{0.7}\text{Ca}_{0.3}\text{MnO}_3$ exhibits logarithmically slow dynamics at all temperatures below T_{SRF} . The system does not reach equilibrium on time scales up to 10^4 s even at temperatures far above T_f . Furthermore, together with the long-time relaxation, aging effects⁷ can also be seen not only below but also well above T_f . Fig. 4 displays the relaxation rates $S(t) = 1/H(\partial m(t)/\partial \log t)$ derived from the ZFC $m(t)$ curves recorded at (a) $T_m = 27\text{K} < T_f$ and (b) $T_m = 45\text{K} > T_f$; $H = 0.1$ Oe and $t_w=0\text{s}$ (10s) and 3000s. The figure shows that $S(t)$ attains a characteristic aging maximum at an observation time close to t_w , where there exists an inflection point in the corresponding $m(t)$ curves; a similar non-equilibrium behavior has been observed in a variety of frustrated and disordered systems including some other perovskite compounds^{1,2,8,9}. In spin-glasses, the aging effect can be interpreted within the droplet model¹⁰ by associating the maximum in the relaxation rate to a crossover between a quasi-equilibrium dynamic regime at short observation times ($t \ll t_w$) and a non-equilibrium regime at long observation times ($t \gg t_w$). Results from Monte Carlo simulations for two- and three-dimensional Ising spin-glass systems also show that the relaxation rate $S(t)$ exhibits a maximum at $t \approx t_w$ ¹¹.

The non-equilibrium dynamics observed at temperatures above T_f is probably caused by random dipolar interactions between the ferromagnetic clusters. In this region, the relaxation time of the system may remain finite although it is much larger than the time scales employed in our experiments. In fact, in original SG systems, aging effects are found also at temperatures above T_g at time scales shorter than the maximum relaxation time of the system¹².

In both two and three dimensional spin glasses, temperature cycling experiments have shown that aging states are virtually unaffected by a negative ΔT , while re-initialization occurs for a sufficiently large positive $\Delta T > 0$ ¹³. On the other hand, for frustrated ferromagnetic systems, re-initialization occurs irrespective of the sign of ΔT ^{8,13,14}. This difference can be used to distinguish a spin glass from other frustrated magnets. $S(t)$ measured at $T_m = 27$ K with $\Delta T=0, -3$ and -5 K and $t_{w2}=0\text{s}$ are indistinguishable from each other, evidencing spin

glass behavior below T_f ; the corresponding experiments above T_f at $T_m = 45$ K give the same result. As shown in Fig. 5 (a) and (b), if a long wait time t_{w2} is added, a small but noticeable reinitialization occurs, in accordance with the behavior of ordinary spin glasses¹⁵. The spin configuration of the aging state at T_m seems to be frozen in as the temperature is lowered. In the positive cycling experiment one notices an increase of $S(t)$ at short time scales indicating re-initialization of the configuration.

At $T > T_f$ (Fig. 5(b)), the $S(t)$ curves measured at 45 K with $\Delta T=0, -3, -5,$ and $+5$ K look very very similar to the $T_m = 27$ K curves. The material still exhibits a characteristic SG behavior, strikingly different from the behavior of a reentrant ferromagnetic phase, which could have been anticipated since we observe ferromagnetic ordering above T_f . However, we deal here with a system that only exhibits short-range ferromagnetic correlation. In passing, it is worth noting that the magnitude of the aging is large below T_{SRF} , proving the effect to be intrinsic to the material rather than only associated to a possible spin disorder at grain boundaries.

B. Ac measurements - memory effects

Fig. 6 shows the (a) in-phase and (b) out-of-phase components of the ac susceptibility vs. temperature for different frequencies. As seen on Fig. 6(b) and insert, the ferromagnetic onset is frequency independent. Below $T \approx 60$ K, the out-of-phase component decreases with decreasing frequency. Further decreasing the temperature, there is a frequency dependent maximum in the in-phase component and a corresponding but more pronounced frequency dependence of the out-of phase component. Using these data it is possible to define a freezing temperature T_f that decreases with decreasing frequency. Employing the position of maximum slope in the out-of-phase component as definition of the freezing temperature at observation time $\tau=1/\omega$, we have analyzed the data according to possible dynamic scaling scenarios. The physically most plausible parameters were obtained using activated dynamics and a finite critical temperature,

$$\ln(\tau) \approx -\left(\frac{1}{T_f}\right) \times [(T_f - T_g)/T_g]^\gamma$$

with $\gamma=0.87$ and $T_g=28.9$ K. However, a microscopic relaxation time of order 1 s was encountered. Analyzing the data according to conventional critical slowing down¹⁷ resulted in rather poor fits. Also, analyses according to Arrhenius or generalized Arrhenius slowing down of the dynamics gave no or unphysical parameters. There are thus strong indications of the existence of a finite phase transition temperature, albeit not necessarily to a conventional low temperature spin glass phase.

To further characterize the low and high temperature regions, memory effects were investigated both below and above T_f using the relaxation of the out-of phase component of the ac susceptibility. When cooling from above T_{SRF} (T_g in a conventional SG case), a halt at constant temperature $T_h < T_{SRF}$ is made during t_h , allowing the system to relax towards its equilibrium state at T_h ; both components of the ac susceptibility then decay in magnitude. In spin glasses, this equilibrated state becomes frozen in on further lowering the temperature, and is retrieved on re-heating the system to T_h . The weak low frequency

ac-field employed in this kind of experiments does not affect the non-equilibrium processes intrinsic to the sample, but only works as a non-perturbing probe of the system. A memory effect is here clearly observed, Fig. 7, not only at $T=27\text{K}$ but, surprisingly, also at 45K . The memory dip appears even more clearly when substrating the references curves as in Fig. 7(b). The insert shows the out-of-phase component of the ac susceptibility recorded vs time at $T=27$ and 45K after direct cooling from above T_{SRF} . As already seen in the memory plot, the relaxation is comparably smaller at $T = 45\text{K}$. One notices that the measured relaxation at both temperatures is larger than in the memory experiment; this is because the ac susceptibility in this case was recorded directly after cooling the system from the reference temperature above T_{SRF} to the measurement temperature.

A superimposed dc field affects the ac susceptibility of spin glasses in a peculiar and significant way. The in-phase component is significantly suppressed, but only at temperatures above the freezing temperature $T_f(H, \omega)$; and the onset of the out-of-phase component is suppressed to lower temperatures, but also remains unaffected at lower temperatures¹⁸! In Fig. 8 we have plotted χ'' in different superposed dc-fields. Fig. 8(a), shows that the near- T_{SRF} magnitude and onset is fragile with respect to even a weak superimposed dc-field. χ'' is substantially affected by a dc-field of only 1 Oe, and is suppressed to lower temperatures already at 5 Oe. At lower temperatures around T_f the out-of-phase component remains unaffected by the dc-field. At larger dc-fields, Fig. 8 (b) shows that also the freezing temperature becomes suppressed, but that the ac susceptibility below T_f remains unaffected in a spin glass like fashion¹⁸.

IV. CONCLUSION

The magnetic response of $\text{Y}_{0.7}\text{Ca}_{0.3}\text{MnO}_3$ becomes governed by short range ferromagnetic correlations at temperatures below $T_{SRF} \approx 70\text{K}$. Above T_f , a surprisingly SG-like state is observed, featuring aging and memory effects. The non-equilibrium dynamics above T_f may be attributed to a thermally activated redistribution of ferromagnetically ordered clusters and the random dipolar interaction amongst their magnetic moments. This state seemingly evolves into a conventional spin-glass state at temperatures below T_f .

ACKNOWLEDGMENTS

Financial support from the Swedish Natural Science Research Council (NFR) is acknowledged. This work is also sponsored by Sida/SAREC - and the ISP of Uppsala University and partially by a Vietnam's Grant on Basic Research. The authors thank Dr. P. V. Phuc and N. D. Van for the x-ray measurements and phase analyses. Special thanks are due to Prof. N. Chau, Dr. N. L. Minh, and Dr. B. T. Cong for their help in sample preparation. The authors are also extremely grateful to Dr. P. Jönsson for her help.

REFERENCES

- ¹ D. N. H. Nam, R. Mathieu, P. Nordblad, N. V. Khiem, and N. X. Phuc, *Phys. Rev. B* **62**, 1027 (2000).
- ² R. Mathieu, P. Svedlindh, and P. Nordblad, *Europhys. Lett.* **52**, 441 (2000).
- ³ X. L. Wang, J. Horvat, H. K. Liu, and S. X. Dou, *J. Magn. Magn. Mater.* **182**, L1 (1998).
- ⁴ L. Sandlund, P. Svedlindh, P. Granberg, P. Nordblad, and L. Lundgren, *J. Appl. Phys.* **64**,5616 (1988).
- ⁵ J. Magnusson, C. Djurberg, P. Granberg, and P. Nordblad, *Rev. Sci. Instrum.* **68**, 3761 (1997).
- ⁶ J. M. De Teresa, M. R. Ibarra, J. Garcia, J. Blasco, C. Ritter, P. A. Algarabel, C. Marquina, and A. del Moral, *Phys. Rev. Lett.* **76**, 3392 (1996).
- ⁷ L. Lundgren, P. Svedlindh, P. Nordblad, and O. Beckman, *Phys. Rev. Lett.* **51**, 911 (1983); L. Lundgren, P. Svedlindh, and O. Beckman, *J. Magn. Magn. Mater.* **31-34**, 1349 (1983).
- ⁸ D. N. H. Nam, K. Jonason, P. Nordblad, N. V. Khiem, and N. X. Phuc, *Phys. Rev. B* **59**, 4189 (1999).
- ⁹ J. Mira, J. Rivas, K. Jonason, P. Nordblad, M. P. Breijo, M. A. Señarís Rodríguez, *J. Magn. Magn. Mater.* **196-197**, 487 (1999).
- ¹⁰ D. S. Fisher and D. A. Huse, *Phys. Rev. B* **38**, 373 (1988).
- ¹¹ J.-O. Andersson, J. Mattsson, and P. Svedlindh, *Phys. Rev. B* **46**, 8297 (1992); H. Rieger, *Physica A* **224** 267 (1996).
- ¹² P. Nordblad, K. Gunnarsson, P. Svedlindh, and L. Lundgren, *J. Magn. Magn. Mater.* **71**, 17 (1987); P. Svedlindh, K. Gunnarsson, P. Nordblad, L. Lundgren, A. Ito, and H. Aruga, *J. Magn. Magn. Mater.* **71**, 22 (1987).
- ¹³ P. Nordblad, in "Dynamical properties of unconventional magnetic systems", Eds. A. T. Skjeltorp and D. Sherrington, Kluwer, 1998, pp. 343-346; P. Nordblad and P. Svedlindh, in "Spin-glasses and Random Fields", Ed. A. P. Young, World Scientific, 1997, pp. 1-27 and references therein; K. Jonason and P. Nordblad, *Eur. Phys. J. B* **10**, 23 (1999).
- ¹⁴ E. Vincent, V. Dupuis, M. Alba, J. Hammann, and J.-P. Bouchaud, *Europhys. Lett.* **50**, 674 (2000).
- ¹⁵ P. Granberg, L. Lundgren, and P. Nordblad, *J. Magn. Magn. Mater.* **52**, 228 (1990).
- ¹⁶ T. Jonsson, K. Jonason, and P. Nordblad, *Phys. Rev. B* **59**, 9402 (1999); C. Djurberg, K. Jonason, and P. Nordblad, *Eur. Phys. J. B* **10**, 15 (1999).
- ¹⁷ P. C. Hohenberg and B. I. Halperin, *Rev. Mod. Phys.* **49**, 435 (1977).
- ¹⁸ J. Mattsson, T. Jonsson, P. Nordblad, H.A. Katori, and A. Ito, *Phys. Rev. Lett.* **74**, 4305 (1995).

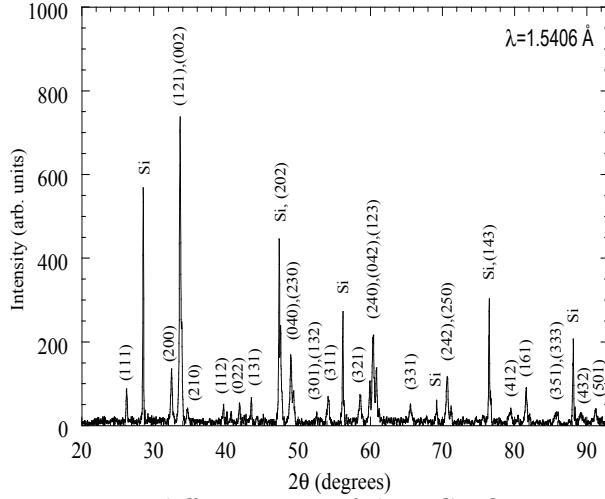


FIG. 1. Room temperature x-ray diffractogram of the YCMO compound mixed with Si powder. The index of the YCMO reflections is added, and the Si peaks identified.

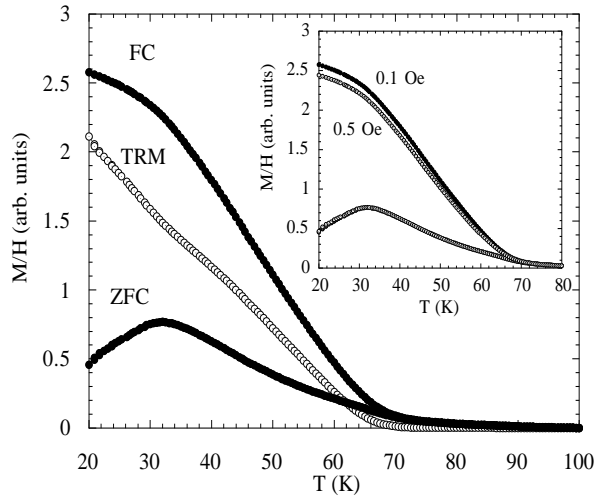


FIG. 2. M_{ZFC}/H , M_{FC}/H , and M_{TRM}/H as functions of temperature using an applied field of 0.1 Oe. The inset shows M_{ZFC}/H and M_{FC}/H at $H=0.1$ Oe and $H=0.5$ Oe.

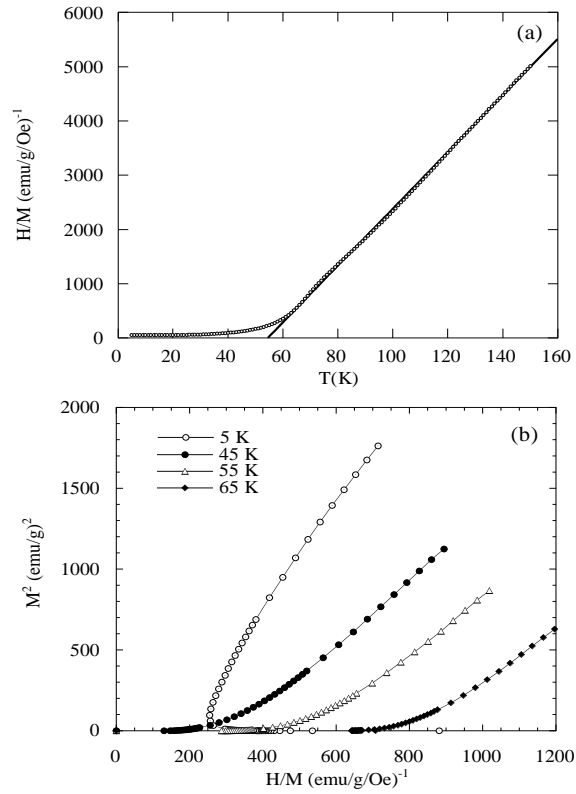


FIG. 3. (a) Curie-Weiss law from magnetization measurements made in a larger field ($H=20$ Oe) up to higher temperatures. (b) Arrot plots of magnetization curves measured at 5, 45, 55, and 65 K.

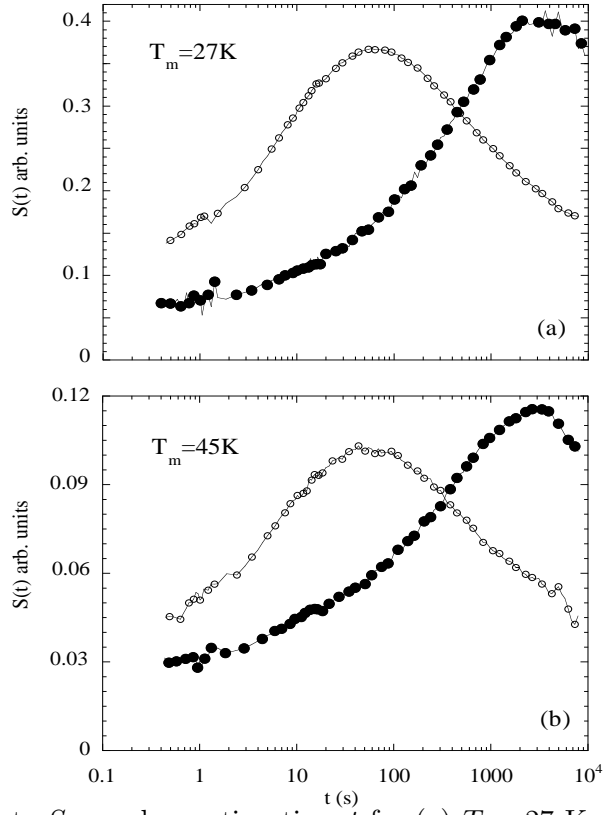


FIG. 4. Relaxation rate S vs. observation time t for (a) $T = 27$ K and (b) $T = 45$ K; results for $t_w = 0$ s (open symbols) and 3000 s (filled symbols) are presented. $H = 0.1$ Oe.

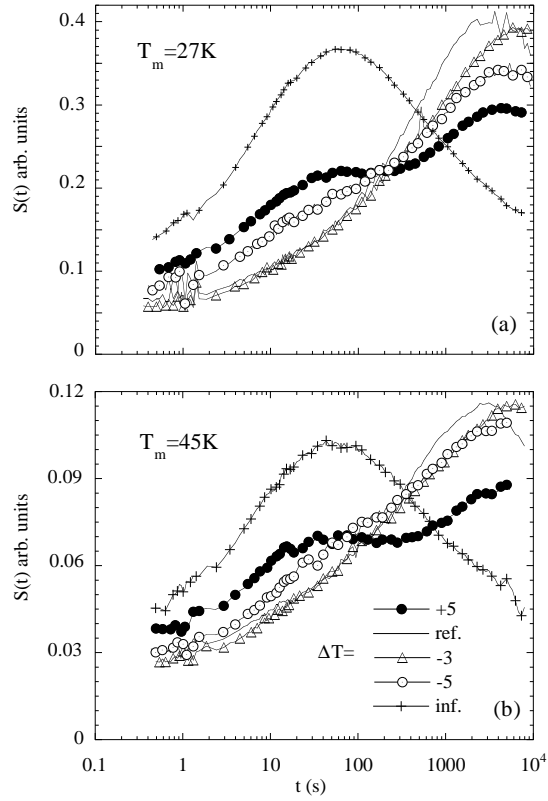


FIG. 5. Relaxation rate S recorded at (a) $T_m = 27$ K and (b) 45 K after positive and negative temperature cyclings. $H = 0.1$ G and $t_{w1}=3000$ s. $t_{w2}=30000$ s for negative cycles; $t_{w2}=0$ s for the positive ones. Infinite ΔT corresponds to $t_{w1}=0$ s.

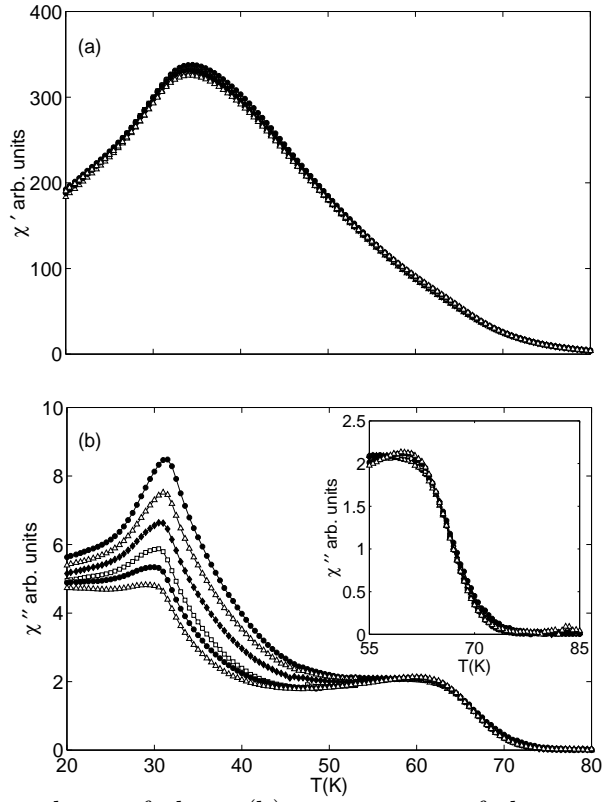


FIG. 6. In-phase (a) and out-of-phase (b) components of the ac susceptibility for different frequencies: 510, 170, 51, 17, 5.1 and 1.7 Hz; $h_{ac}=0.01$ Oe. The insert shows an enlargement of the 55-85K region.

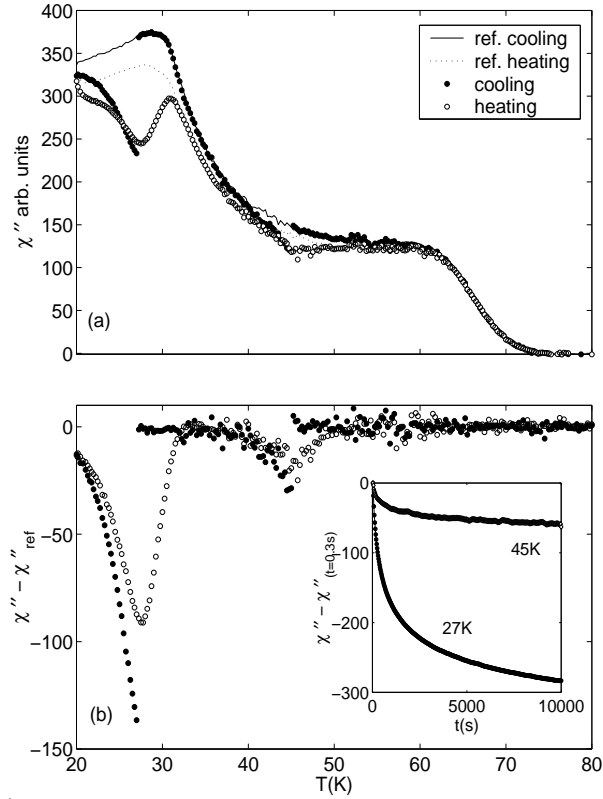


FIG. 7. (a) χ'' and (b) $\chi'' - \chi''_{ref}$ vs. temperatures measured during cooling (filled circles and line) or on re-heating (open circles and dotted line). In the case of the curve with filled circles, the sample was kept 10000s at 45 and 27K during cooling. The insert shows the corresponding relaxation of $\chi'' - \chi''_{(t=0.3s)}$ vs. time.

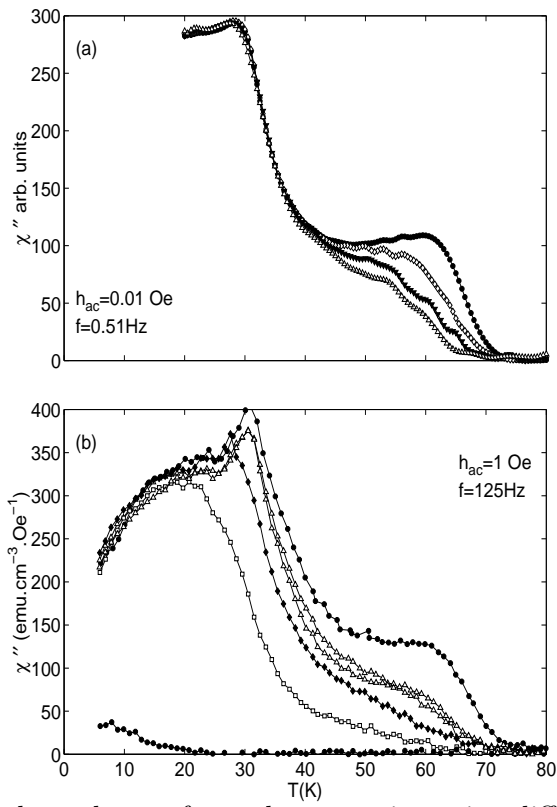


FIG. 8. Temperature dependence of χ'' when superimposing different dc fields. (a) shows the results for small dc fields: 0,1,2 and 5 Oe; (b) for high ones: 0,10,100,300,1000 and 10000 Oe.